

Innovative Solutions Improve Transmission Line Protection

Daqing Hou, Armando Guzmán, and Jeff Roberts
Schweitzer Engineering Laboratories, Inc.

Presented at the
1998 Southern African Conference on Power System Protection
Midrand, South Africa
November 3–4, 1998

Previously presented at the
12th Annual CEPSI Exhibition, November 1998,
1998 International Conference Modern Trends in the Protection Schemes of Electric
Power Apparatus and Systems, October 1998,
and 52nd Annual Georgia Tech Protective Relaying Conference, May 1998

Originally presented at the
24th Annual Western Protective Relay Conference, October 1997

INNOVATIVE SOLUTIONS IMPROVE TRANSMISSION LINE PROTECTION

Daqing Hou, Armando Guzmán, Jeff Roberts
Schweitzer Engineering Laboratories, Inc.
Pullman, WA USA

INTRODUCTION

Transmission line protection depends upon a core group of protective elements. These elements must be dependable and secure for all power system conditions as any single weakness can cause problems with a relaying scheme.

Some common concerns related to a line distance relay are operating speed, load and fault impedance induced element under- and overreach, out-of-step (OOS) conditions, and Capacitive Voltage Transformer (CVT) transients. This paper presents the following innovative solutions to overcome these concerns:

- Variable filtering algorithm that improves operating speed without sacrificing security.
- Adaptive polarizing scheme that accommodates rapidly changing system conditions.
- Adaptive logic that discriminates between faults and OOS conditions.
- Secure Zone 1 distance element that does not overreach due to CVT transients.
- Secure means to decrease total protection tripping times in communications-aided tripping schemes.

VARIABLE FILTERING REDUCES DISTANCE PROTECTION TRIPPING TIME

To provide protection security and dependability, protective relays must filter their input voltages and currents to obtain reliable relaying quantities. Distance relays utilize the fundamental frequency components of voltages and currents. For these relays, all quantities other than the fundamental component are noise.

The noise involved in the relaying voltages and currents determines the degree of filtering needed to accurately extract the fundamental components for impedance calculations. Table 1 contains a list of possible noise contamination to the relaying voltages and currents. This table also lists the type of filtering needed for each type of noise.

Table 1: Noise Contained in Relaying Voltage or Current and the Filtering Required to Remove the Noise

Noise	Cause	Voltage	Current	Filtering
Decaying DC	Short circuit faults	No	Yes	Double differentiator
Trap charge	Line open after a fault	Yes	No	Differentiator
CVT transient	Bad CVT response	Yes	No	Highpass
Subfundamental freq.	Series capacitor compensation	Yes	Yes	Highpass
Even harmonics	CT saturation, etc.	Very little	Yes	One-cycle window or longer
Odd harmonics	Arc furnace, nonlinear apparatus	Yes	Yes	Half-cycle window or longer
High frequency noise	Traveling waves, capacitor switching, etc.	Yes	Yes	Lowpass

A one-cycle Fourier filter plus a differentiator (also called a digital transactor or digital mimic) or a one-cycle cosine filter are effective bandpass filters which reject most types of noise listed in Table 1. These two filters are indeed the most popular filtering techniques used in modern microprocessor relays. Compared to the one-cycle cosine filter, the Fourier filter plus a differentiator sacrifices some high-frequency noise rejection capability to gain a little speed advantage.

Distance relay accuracy is important when a fault lies at the limits of zone reach settings. Accuracy assures that the relay does not overreach to the next protection zone and therefore guarantees coordination of the overall protection scheme. Accuracy is less important for close-in faults where overreach is unlikely.

A typical tripping speed curve of a protective relay, as shown in Figure 1, demonstrates the relationship between fault location and tripping speed. Protective relays are expected to trip fast for close-in faults in strong systems. The reduced tripping time for close-in faults is pronounced for strong systems or systems with low System Impedance Ratios (SIR). The tripping speed is almost constant for high SIR systems because fault current does not increase significantly for faults closer to the source. Figure 1 includes a speed curve for a variable filtering technique that will be discussed later in this section.

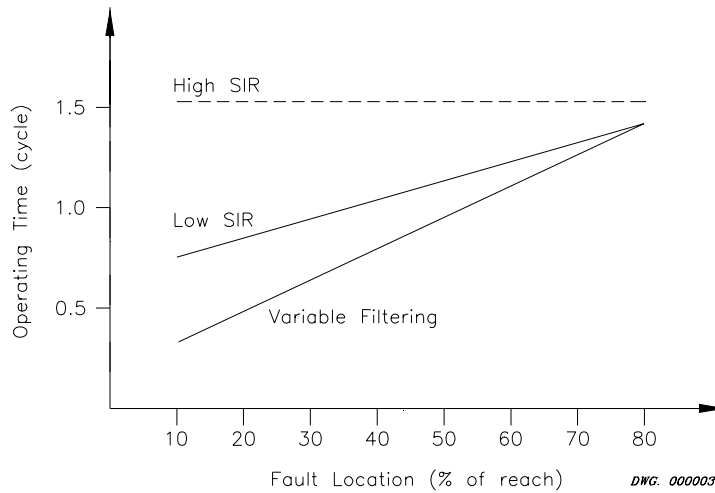


Figure 1: Typical Distance Relay Speed Curves

Reference [1] shows the relationship between relay sampling rate and Zone 1 element operating time. Figure 2 shows that increasing the sampling rate from 16 to 32 samples per cycle yields a reduction of about 1/32-cycle in operating time or 0.5 ms for a 60 Hz system. This negligible operating time reduction is achieved at an expense of double computational burden. Above a sufficiently high sampling rate, the digital filtering window length is the determining factor of the element operating speed. To further reduce the fault clearance time for close-in faults, a digital filter with less than a one-cycle window is necessary.

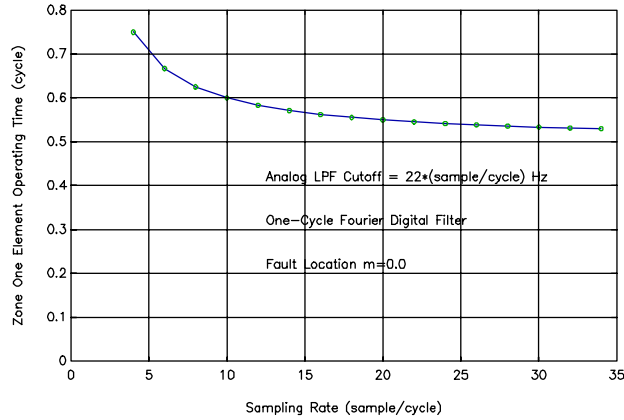


Figure 2: Operating Time vs. Sampling Rate

The filters discussed so far are Finite Impulse Response (FIR) filters. The filtering capability of an FIR filter largely depends on its window length, which is defined as the length of input data that the filter uses to calculate its output at any given time. An FIR filter with less than a one-cycle window cannot reject all harmonics; especially the lower harmonics. For example, the half-cycle cosine filter has little attenuation at the second harmonic, as shown by its frequency response plot in Figure 3. The filter effectiveness in removing noise from relaying quantities directly influences the accuracy of fault impedance calculations. To successfully use shorter filters to speed-up distance elements, we have to understand quantitatively how filter window length influences relaying accuracy.

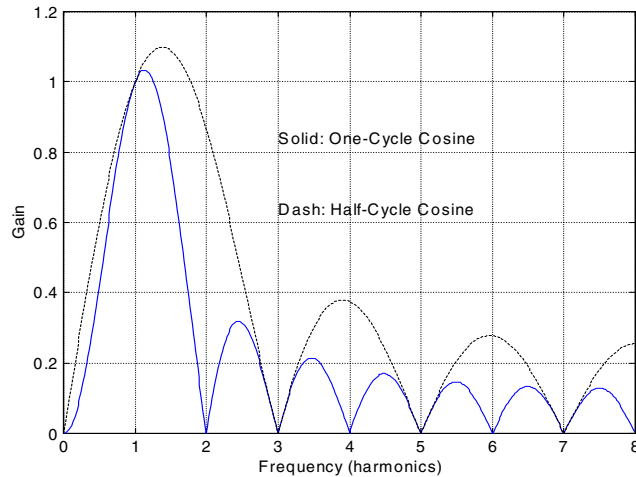


Figure 3: Frequency Responses of Half- and One-Cycle Cosine Filters

Reference [2] presents a study of the statistical relationship between the impedance calculation accuracy and filter window length. The study used a random error signal with a power spectrum density determined from an extensive fault simulation on a power system model. The general relationship between the impedance calculation error and the filtering window is shown in Figure 4. Notice that this study did not include some common sources of error such as DC offset, CT saturation, CVT transients, and series-compensation capacitor induced sub-fundamental frequencies. Nevertheless, the graph shown in Figure 4 provides a guideline to reduce the distance element reach setting to avoid overreach when the filter window is shorter than one cycle.

With a one-cycle filtering window, the maximum impedance calculation error is approximately 8% of the line impedance as shown in Figure 4. This error, plus a CT and PT ratio mismatch, inaccurate line parameters, etc., dictates a usual Zone 1 reach setting of 80-85% of the line impedance. When the filtering window decreases to one-half cycle, Figure 4 shows a reach reduction of another 10%. The reach setting for a quarter-cycle-window filter should be reduced by an additional 20% as indicated by Figure 4.

When using a CVT, we need to add the CVT-transient-induced impedance calculation error to those errors shown in Figure 4. There are two ways to cope with the CVT error for a given filtering scheme. One is to have a fixed, additional reach reduction according to the error added by CVTs. This fixed reach reduction slows down relay operating speed for all system configurations. The other method is to use an adaptive reach. We shall describe later how to estimate system SIRs to adaptively adjust the protection reach to avoid the CVT-transient-induced distance element overreach.

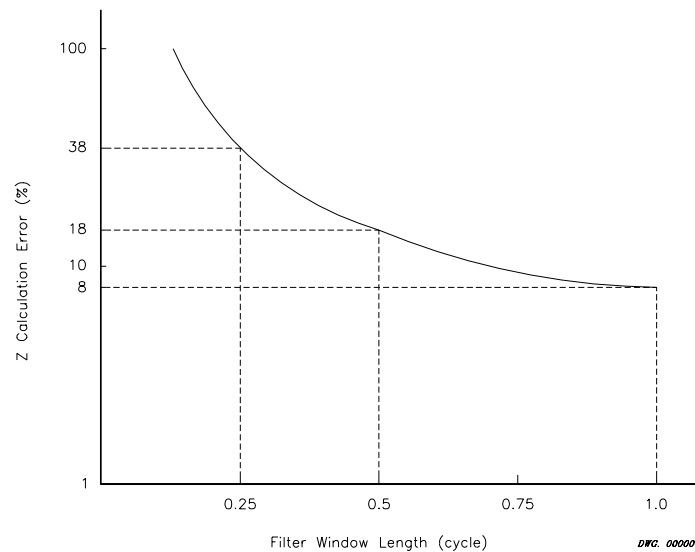


Figure 4: Calculated Impedance Accuracy vs. Filtering Window Length

To decrease the distance element tripping time for more critical close-in faults, a variable filtering and reach comparison scheme is proposed in Figure 5. The impedance calculation using the full-cycle window is compared directly against the full reach setting since this calculation is the most accurate. The impedance calculation using the quarter-cycle filtered data is compared to a much reduced reach setting to guarantee that it does not overreach Zone 1, even though the calculation involves many uncertainties. We can take advantage of the symmetry of the one-cycle cosine filter by cascading quarter-cycle filters.

Relay tripping speed using the variable filtering scheme is shown in Figure 1. As expected, the relay quickly detects the close-in faults but still retains its high accuracy, and therefore security, for faults near the end of line.

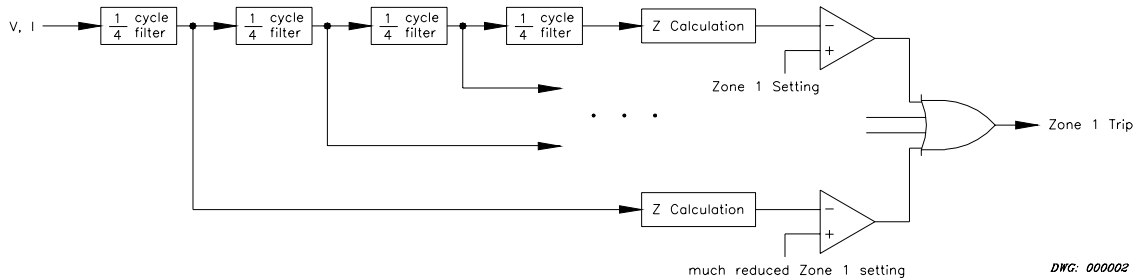


Figure 5: Variable Filtering Scheme

POLARIZING SCHEME ADAPTS TO CHANGING SYSTEM CONDITIONS

Comparator-based mho elements require a polarizing quantity to provide a reliable angle reference. When a fault occurs, this angle reference should be stable and last long enough to guarantee that the protection element consistently picks up until the fault is cleared. The following are basic requirements for the polarizing quantity [3]:

- Provide reliable operation for all in-zone faults.
- Be secure for all external faults.
- Provide stable operation during single-pole open conditions.
- Tolerate fault resistance.

There are many different kinds of polarizing quantities, that can be categorized as follows:

- **Self-polarization** - uses the faulted phase loop voltage as a polarizing quantity. The resulting mho characteristic is often referred to as a static mho because it does not change with system conditions, fault conditions, or time.
- **Cross-polarization** - uses healthy phase (nonfaulted) loop voltages as the polarizing quantity. The mho characteristic produced is called a variable mho due to its variable shapes for different system and fault conditions. The cross-polarized mho characteristic does not change with time.
- **Memory-polarization** - uses memorized self- or cross-polarizing quantities as a polarizing quantity. The mho characteristic produced by memory polarization is a so-called dynamic mho because the mho characteristic size changes as the memory dies out with time.
- **Combined-polarization** - the most popular combined polarizing scheme is positive-sequence voltage polarization with memory. The positive-sequence voltage itself provides a combination of self- and cross-polarization.

Self-polarization is the oldest and simplest type of polarization. It has many disadvantages. Self-polarization does not have enough fault resistance coverage, is insecure for external faults with certain load flow and fault resistance, and does not work for zero-voltage faults.

Cross- and memory-polarization expand the mho characteristic all the way back to the local source impedance. This characteristic expansion provides greater fault resistance coverage (especially for weaker local source systems). These polarizing techniques also make the characteristics adapt to load flow to avoid heavy load-flow induced overreach.

Although cross-polarization improves fault-resistance coverage and security, it still does not work for the zero-voltage three-phase faults. A memory function is necessary to provide reliable fault detection for zero-voltage three-phase faults.

Some common types of memory polarizing techniques are Infinite Impulse Response (IIR) filtering or rotating registers for microprocessor relays or parallel resonant circuits for solid-state relays. Equation 1 shows an IIR filter used as polarizing memory in a microprocessor relay. The constant α controls memory length (a smaller α gives longer memory).

$$V_{I_{mem\ k}} = \alpha \cdot V_{1k} - (1 - \alpha) \cdot V_{I_{mem\ k-halfcycle}} \quad \text{Equation 1}$$

$$\alpha < 1$$

where: V_{1k} is present positive-sequence voltage value
 $V_{I_{mem\ k}}$ is present memorized positive-sequence voltage value
 $V_{I_{mem\ k-halfcycle}}$ is half-cycle old memorized positive-sequence voltage value

The choice of memory time constant or the length of polarizing memory is always a critical design issue. Considerations in choosing the time constant should include,

- The maximum clearance time of both internal and external zero-voltage faults.
- Backup-zone fault clearance time on high SIR systems where the relaying voltage might be very small even for remote faults.
- Bypass-switch operating time of series-compensation capacitors.

On series-capacitor compensated lines, the possibility of voltage inversion exists. Voltage inversion endangers the directional security of the mho distance elements. In such applications, the polarizing memory should be long enough to provide correct and consistent distance element operation until the fault is cleared, the spark-gap protection operates, or the capacitor bypass switch operates to clear the voltage inversion. A typical polarizing memory time is between 3 and 20 cycles.

A longer polarizing memory helps to detect faults in difficult system and fault conditions like those mentioned above. However, longer memory also comes with a serious security drawback when there is a system frequency excursion. Power system disturbances are often accompanied by a frequency excursion. As an example, one North American utility specifies a possible 9 Hz per second rate-of-frequency change. The protective relays must be secure during this frequency excursion.

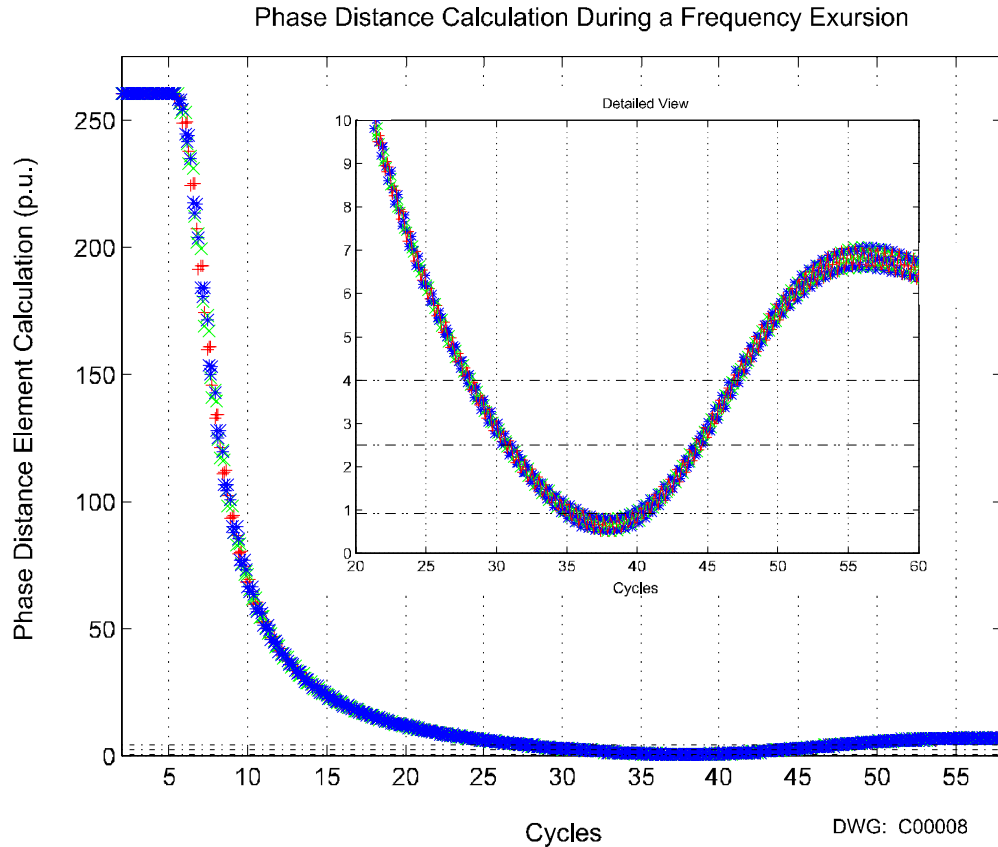


Figure 6: Reach Calculation of Phase Mhos During a Frequency Excursion

Figure 6 shows the long polarizing memory problem during a minus 9 Hz per second frequency excursion after Cycle 5. Note that no fault is present on the monitored line. The vertical axis shows the distance calculation normalized to the line length. The distance calculation of 260 per unit before Cycle 5 is due to load flow on the system. Approximately 30 cycles after the initial frequency excursion occurs, we see that the distance calculation dips below 85% of the line impedance which is the normal Zone 1 distance reach setting. Therefore, the relay would inadvertently trip due to the frequency excursion and the use of a long polarizing memory.

Why did the mho element operate during this frequency excursion? To answer this question, let us review the operation principle of a mho element. A mho element tests the angle between an operating quantity, $Z_R I-V$, and the polarizing quantity, V_{PMEM} . When a fault occurs at the limits of the reach setting, this angle is 90° . The points defined by the 90° relation constitute a circle, within which the operating region is defined. This angle is less than 90° if the fault is inside the operating region.

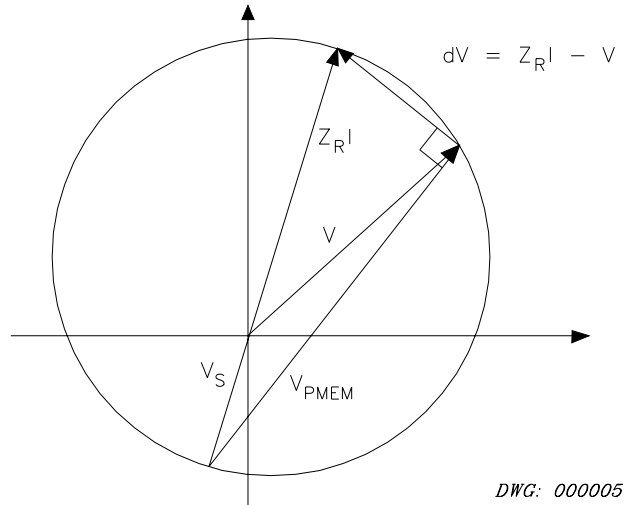


Figure 7: Development of Cross- or Memory-Polarized Mho Characteristic

When a frequency excursion occurs, the mho distance relay tracks to the new frequency. Due to the memory effect, the polarizing voltage phase angle starts to slip away from the input voltage phase angle and a phase angle difference results as shown in Figure 8. If this frequency excursion persists long enough, the angle difference between $Z_{R}I-V$ and V_{PMEM} becomes less than 90° as shown in Figure 9b.

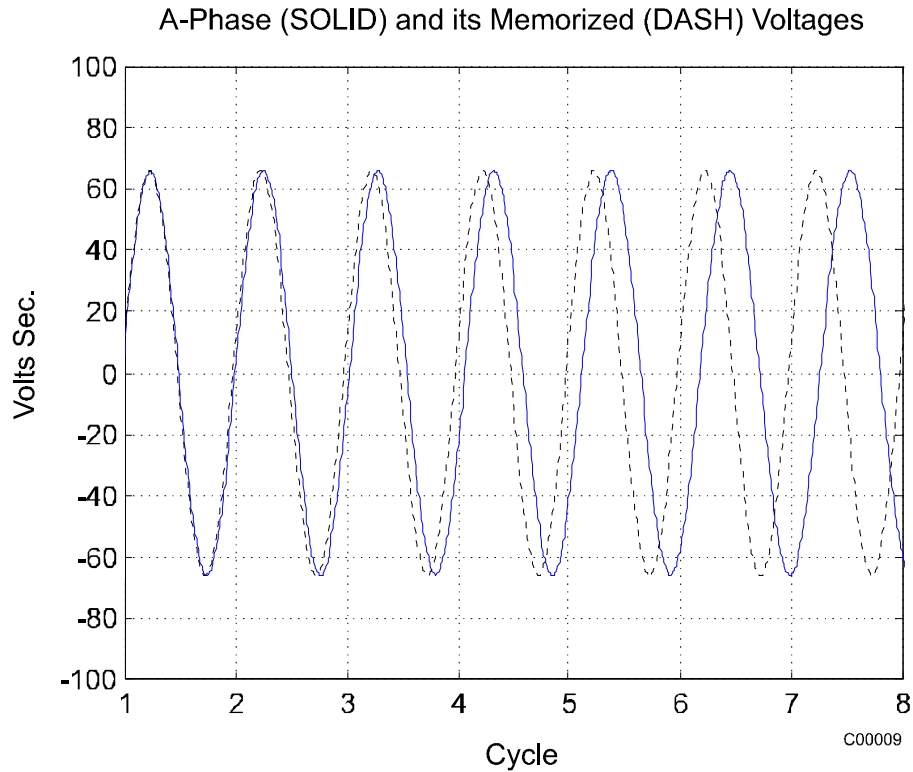


Figure 8: Polarizing Quantity Slips Away From the Voltage Inputs

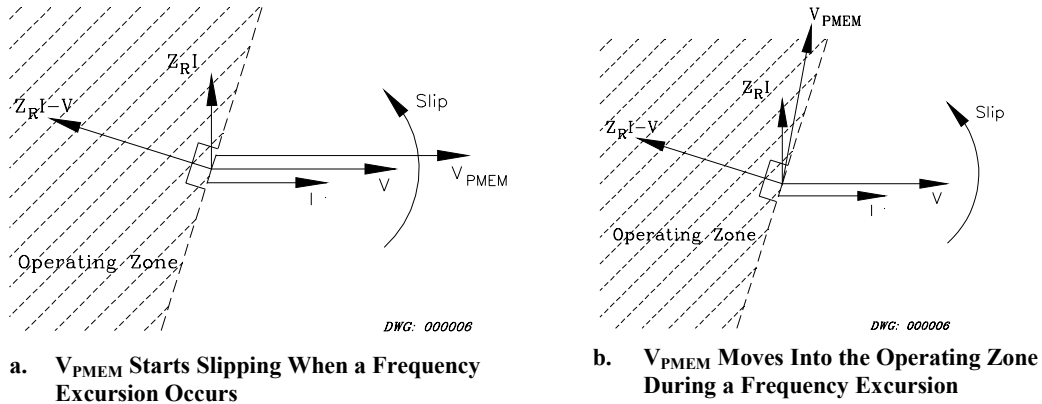


Figure 9: Polarizing Quantity Slips into Operating Zone

To overcome the long polarizing memory problem and at the same time provide a reliable polarizing quantity for zero-voltage faults and faults with a voltage inversion, we use an adaptive polarizing scheme as shown in Figure 10. Using the adaptive polarizing scheme, the relay normally uses the positive-sequence voltage (V_1) with little or no memory for the polarizing quantity. This polarization works satisfactorily for all faults other than zero-voltage three-phase faults and faults with a voltage inversion. When the relay detects that V_1 is less than a predetermined magnitude or the relay detects a voltage inversion, it switches to a long-memory V_1 polarizing quantity.

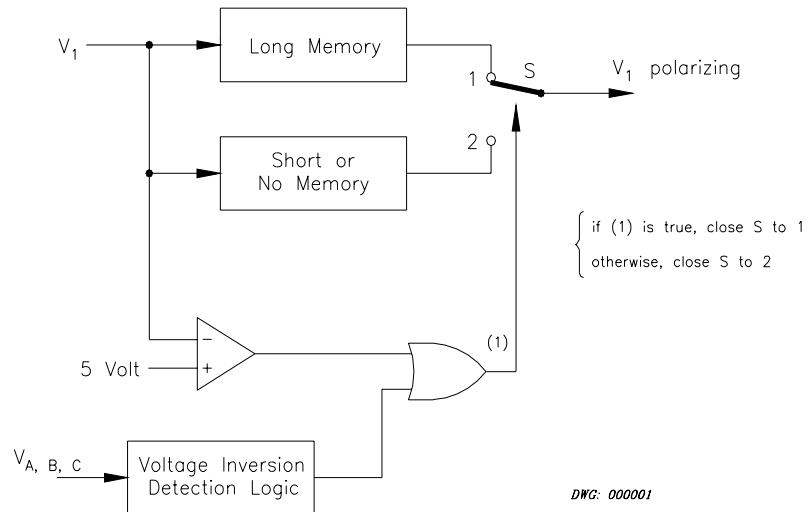


Figure 10: Adaptive Polarizing Scheme

Figure 11 shows the results of using adaptive polarizing memory for the same disturbance as shown in Figure 6. We see that the minimum distance calculation due to the disturbance is around 130 per unit of reach, far away from the Zone 1 tripping zone. The relay therefore restrains successfully for the frequency excursion.

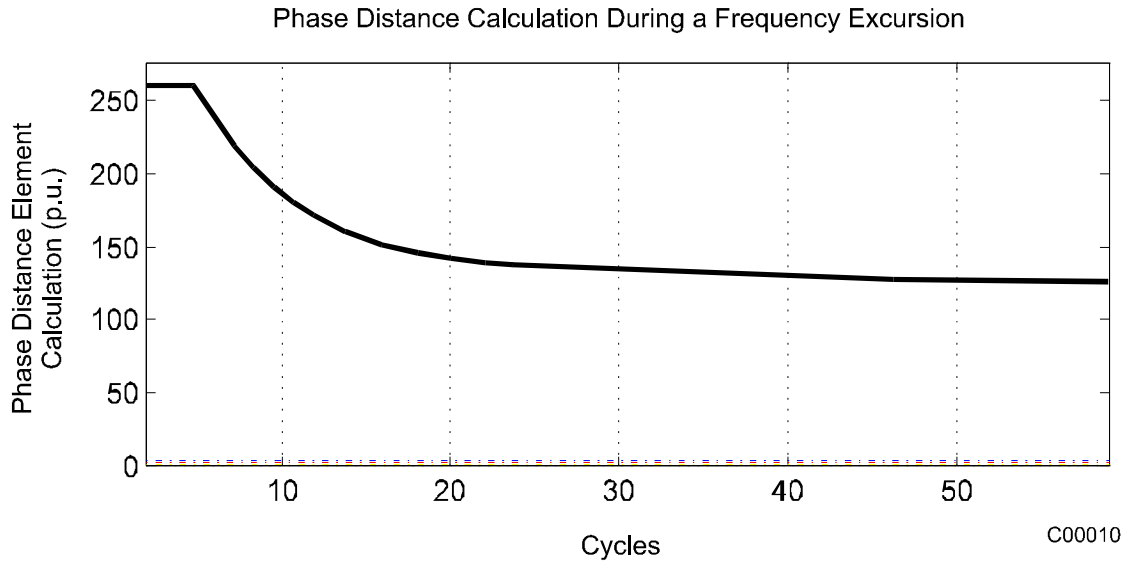


Figure 11: Minimum Reach Calculation of Phase Mhos Using a Short Memory Time Constant

ADAPTIVE OUT-OF-STEP SCHEME INCREASES LINE PROTECTION RELIABILITY

Traditional out-of-step (OOS) detection relays measure the positive-sequence apparent impedance, Z_{λ} , and compare it against two concentric distance element characteristics. The relay detects an OOS condition if Z_{λ} stays inside the outer characteristic and outside the inner characteristic longer than a preset time.

A typical problem of traditional OOS detection relays is that once the relay decides to block the distance elements during OOS conditions, the distance elements cannot detect three-phase faults while Z_{λ} is inside the outer characteristic. This limitation compromises the power system integrity when three-phase faults occur during power swings.

Improving the Dependability of Traditional Distance and OOS Schemes

Traditional OOS blocking schemes lack dependability for three-phase faults during swings. Figure 12 shows an OOS scheme with additional inner blinders, R1. With the inner blinders and the capability to measure the slip frequency when Z_{λ} passes through the outer (R6) and the inner (R5) blinders, the traditional distance schemes can detect three-phase faults during power swings.

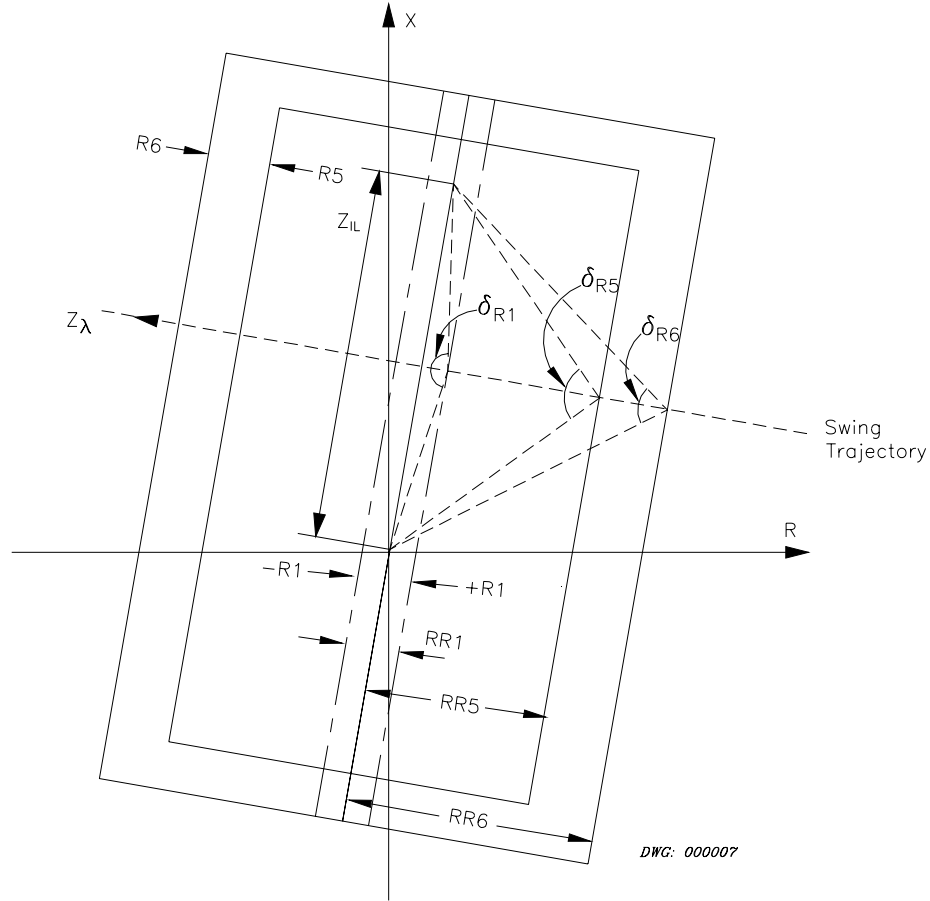


Figure 12: Traditional OOS Characteristic With the Additional Inner Blinders Improves Distance Scheme Dependability

In Figure 12, R5 and R6 define the blinders that the relay uses to measure the slip frequency. The new OOS scheme measures the time for Z_λ to cross between the R6 and R5 blinders, Δt_{R5R6} . With the Δt_{R5R6} information, the relay determines the maximum time for Z_λ to cross between the inner R1 blinders, Δt_{R1} . In the event of a three-phase fault, Z_λ remains inside the R1 blinders longer than Δt_{R1} time. When this happens, the relay resets its OOS blocking condition, allowing the distance elements to trip. Equations 2 and 3 show how to calculate Δt_{R1} .

$$\Delta t_{R1} = \frac{\Delta \delta_{R1}}{\Delta \delta_{R5R6}} \cdot \Delta t_{R5R6} \quad \text{Equation 2}$$

where:

- $\Delta \delta_{R1}$ Load angle difference when crossing between the inner R1 blinders
- $\Delta \delta_{R5R6}$ Load angle difference when crossing between the R5 and R6 blinders, $\delta_{R5} - \delta_{R6}$

$$\Delta t_{R1} = \frac{\pi - 2 \cdot \tan^{-1}\left(\frac{|Z_{1L}|}{2 \cdot RR1}\right)}{\tan^{-1}\left(\frac{|Z_{1L}|}{2 \cdot RR5}\right) - \tan^{-1}\left(\frac{|Z_{1L}|}{2 \cdot RR6}\right)} \cdot \Delta t_{R5R6} \quad \text{Equation 3}$$

where:

- Z_{1L} Positive-sequence line impedance
- RR1 Distance from Z_{1L} to R1
- RR5 Distance from Z_{1L} to R5
- RR6 Distance from Z_{1L} to R6

The need to adapt the Δt_{R1} decision time is shown in Figure 13. The figure shows the phase currents after a single-line-to-ground fault at 0.2 seconds. As we can see from the modulated signal in this figure, the slip frequency is not constant during the OOS conditions. The frequency changes slowly for approximately one second after the fault inception. After one second, the slip frequency changes quickly. In order to determine how long Z_{λ} remains inside the inner blinders, the relay needs to follow changes in the slip frequency as closely as possible. For this reason, the relay updates Δt_{R1} every time Z_{λ} crosses the R6 and R5 blinders.

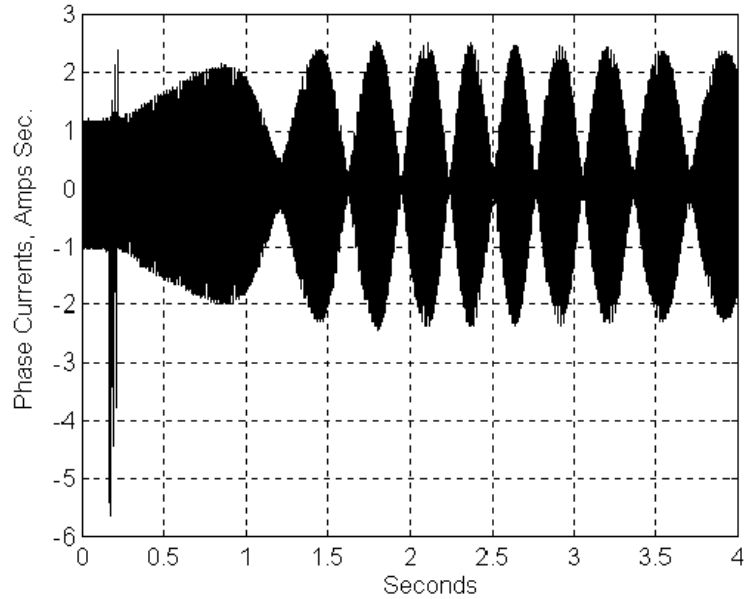


Figure 13: Phase Currents After an SLG Fault Show the Slip Frequency Variations During the Swing Conditions

Relay Performance Under Actual OOS Conditions

The positive-sequence voltage and current for an actual OOS condition obtained from a power system simulator are shown in Figure 14. The modeled system is a single line connecting two generators. The oscillograms show that the OOS condition evolves to a three-phase fault at Cycle 30. These system conditions challenge the traditional OOS schemes. Let us find out why.

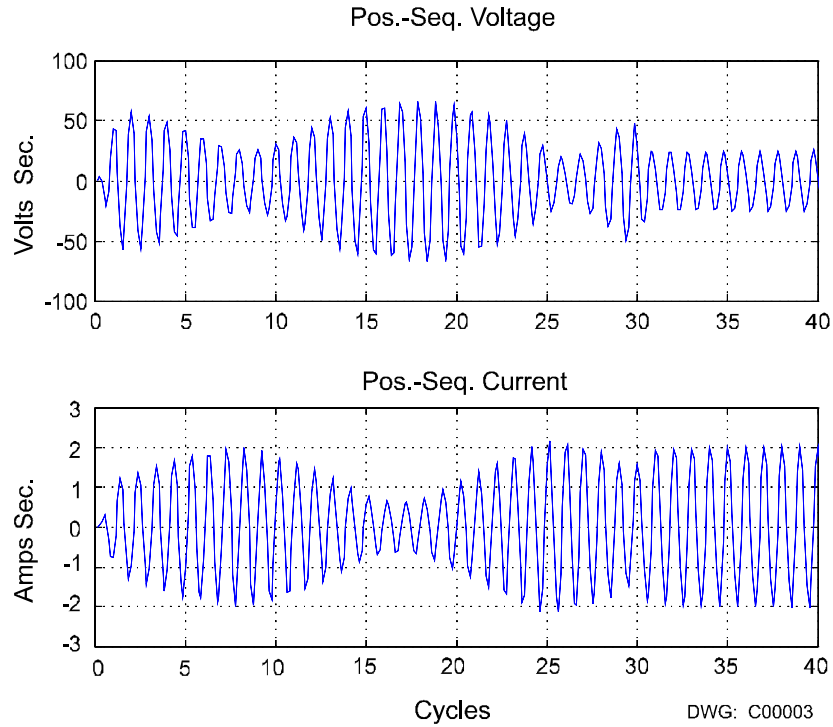


Figure 14: Positive-Sequence Voltage and Current for an Actual OOS Condition That Evolves to a Three-Phase Fault

We can see in Figure 15 the Z_{λ} trajectory during OOS conditions and Z_{λ} after the three-phase fault occurs. Notice that the fault may happen at any point in the trajectory of Z_{λ} . If the fault occurs while Z_{λ} is inside the Zone 6 characteristic, the relay continues to block the distance elements. Therefore, the distance elements cannot detect the fault.

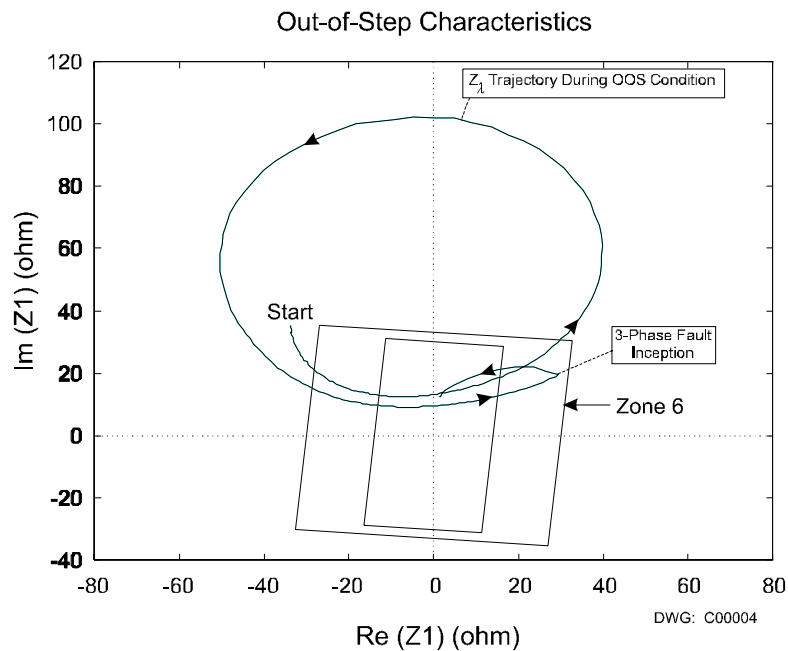


Figure 15: Z_{λ} Trajectory During OOS Condition That Evolves to a Three-Phase Fault

The performance of the OOS relay that uses the additional R1 blinders is shown in Figure 16. We can see that the swing trajectory starts outside Zone 6 and crosses the R6 and R5 blinders from left to right. After crossing R6 and R5, the relay calculates Δt_{R1} according to Equation 3. The relay resets Δt_{R1} when Z_λ is outside the outer characteristic, Zone 6. After the swing completes a cycle, Z_λ crosses the R6 and R5 blinders again and the relay calculates the new Δt_{R1} value. Z_λ continues its trajectory and crosses the inner blinders and the right-hand R5 blinder. After crossing the R5 blinder, the three-phase fault occurs. Then, Z_λ enters the R1 blinders and stays there until the relay unblocks the distance elements. The relay performance under these conditions clearly shows the benefit of adding the R1 blinders and the adaptive timer.

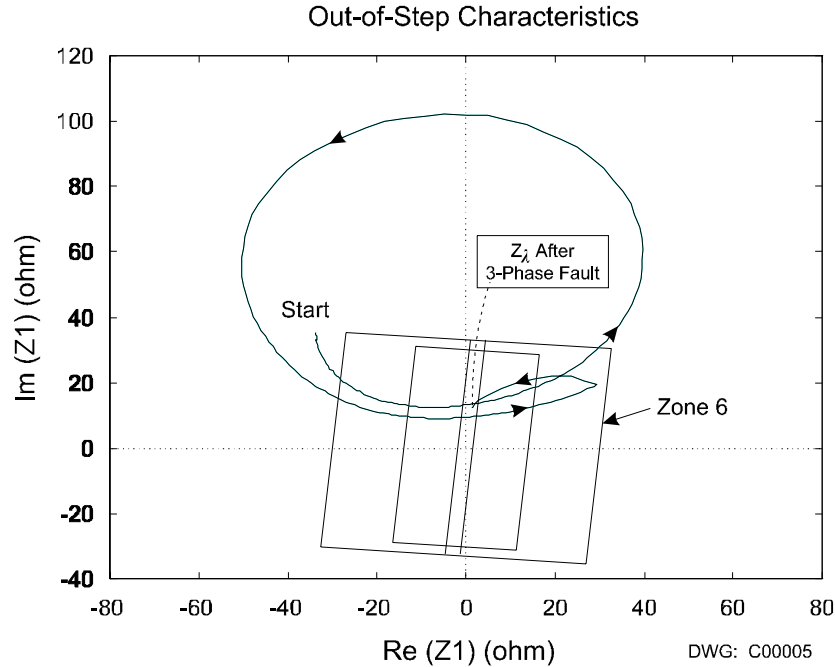


Figure 16: Z_λ Remains Inside R1 Blinder After the OOS Condition Evolves to a Fault

SECURE DISTANCE ELEMENTS DURING CVT TRANSIENTS

Reference [4] discusses the overreach problems of distance elements when using CVTs. Previous solutions assume fixed values of SIR in their logic to reduce the reach of the instantaneous distance elements. With fixed SIR values, the relay may not properly reduce the distance element reach or add unwanted delays for changing system conditions. A new solution provides an accurate reach reduction based on a measured SIR. When a fault occurs, the relay calculates the positive-sequence source impedance, Z_{S1} , with the current and voltage information. It then calculates SIR, which is the ratio of Z_{S1} to the relay reach impedance, Z_{R1} . Figure 17 shows required reach reduction for different SIR values. With this new approach, the relay automatically reduces the reach of the instantaneous portion of the Zone 1 distance element according to the measured SIR. The remainder of the Zone 1 distance element reach is delayed (t_{DELAY}) to allow the CVT transient to disappear (see Figure 18).

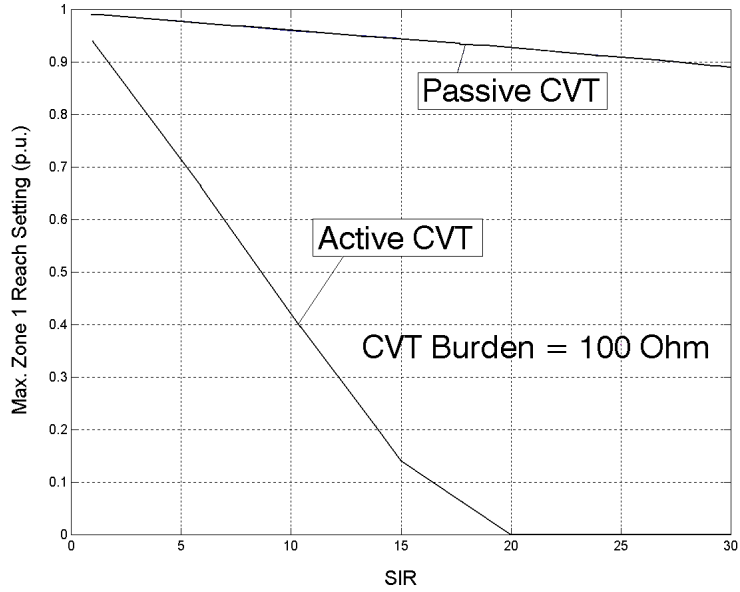


Figure 17: Distance Element Reach Reduction as Function of SIR When Using CVTs With Active or Passive Ferroresonant Suppression Circuit

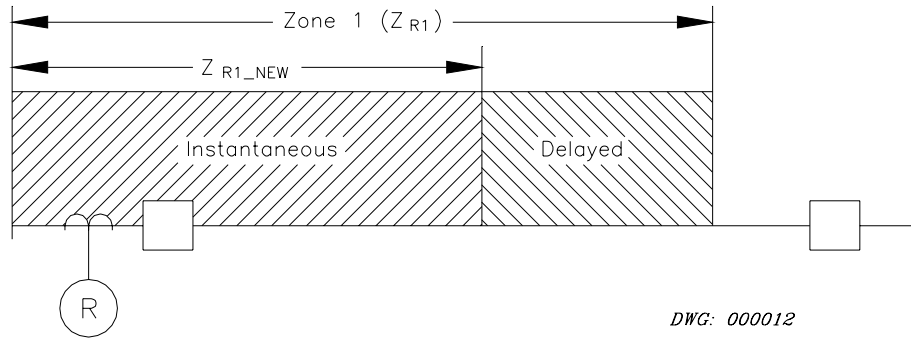


Figure 18: Zone 1 Reach Reduction According to SIR

The first step to determine the required reach reduction is to calculate the source impedance, Z_{S1} . The relay calculates SIR with the source impedance information and the instantaneous element reach. SIR is the input to the chart shown in Figure 17 that characterizes the CVT. The output of the chart is the new relay reach of the instantaneous distance element, Z_{R1_NEW} . Figure 19 summarizes the sequence which determines the amount of reach reduction of the instantaneous distance elements.

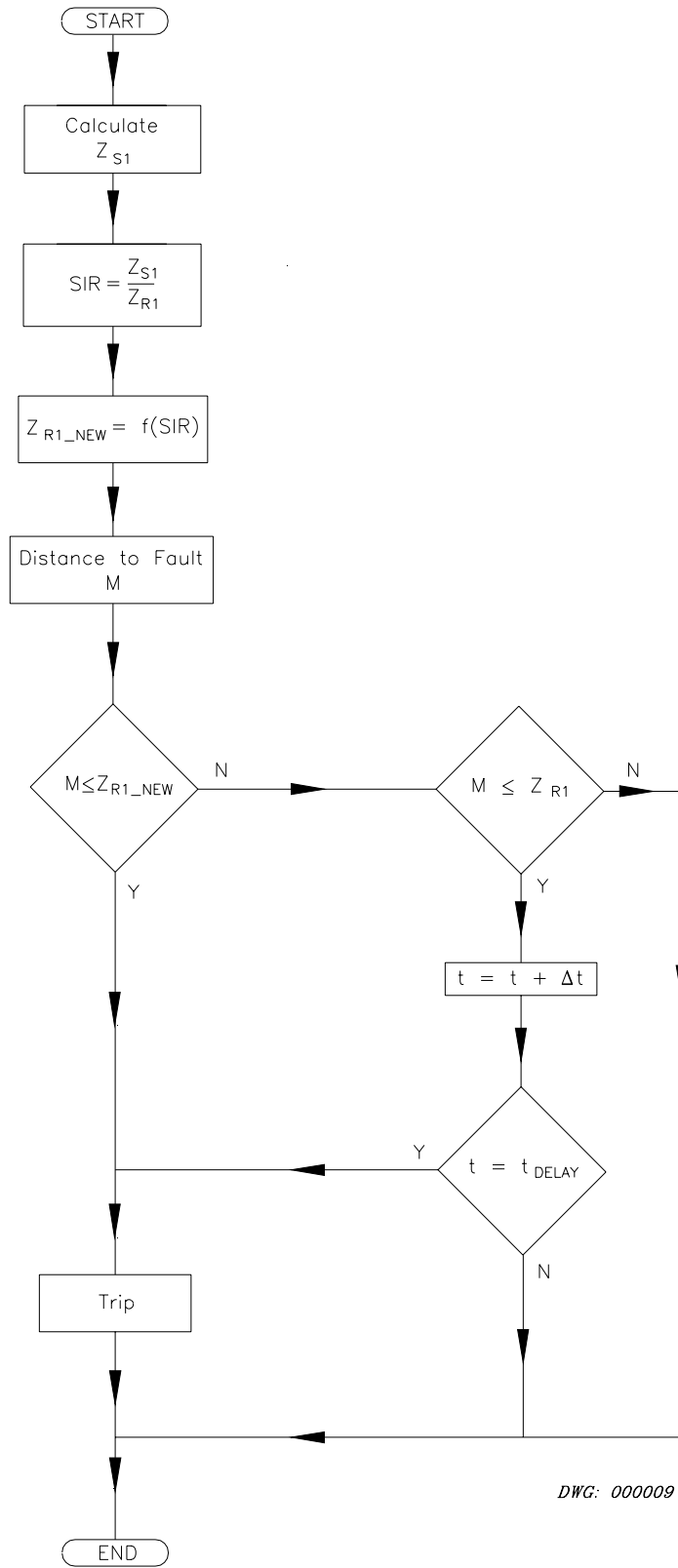


Figure 19: Relay Sequence to Determine the Distance Element Reach Reduction

SIR Calculations Under Actual Fault Conditions

The oscillogram for an A-phase-to-ground fault is shown in Figure 20. The fault is at the end of the instantaneous element reach in a system with $SIR = 10$. Notice that the voltage signal shows the transient due to the CVT response when the fault occurs. This transient causes a relay overreach problem if the relay does not properly reduce its reach.

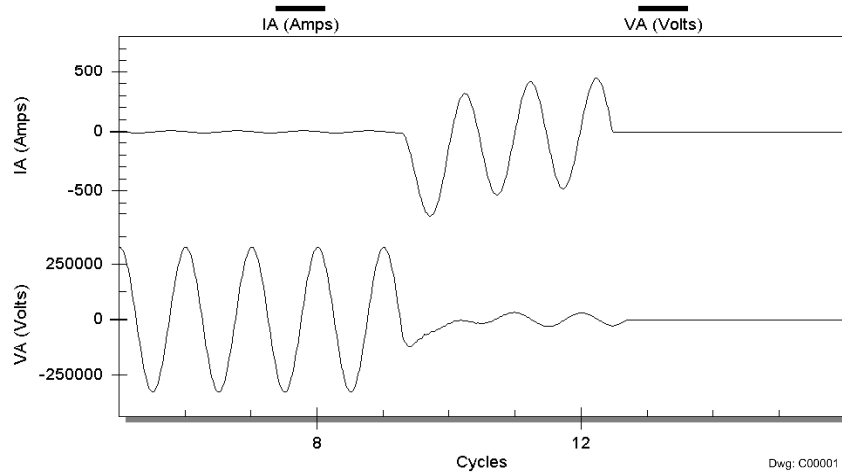


Figure 20: A-Phase Current and Voltage for an A-Phase-to-Ground Fault at the End of Zone 1 in a System with $SIR = 10$

Figure 21 shows the relay SIR calculation for the A-phase-to-ground fault. The calculated SIR after the fault occurrence is approximately 10; the results match the actual SIR. These results show that the SIR calculation provides reliable information to properly reduce the Zone 1 reach. With the new approach, the relay reduces the instantaneous distance element reach according to changing system conditions.

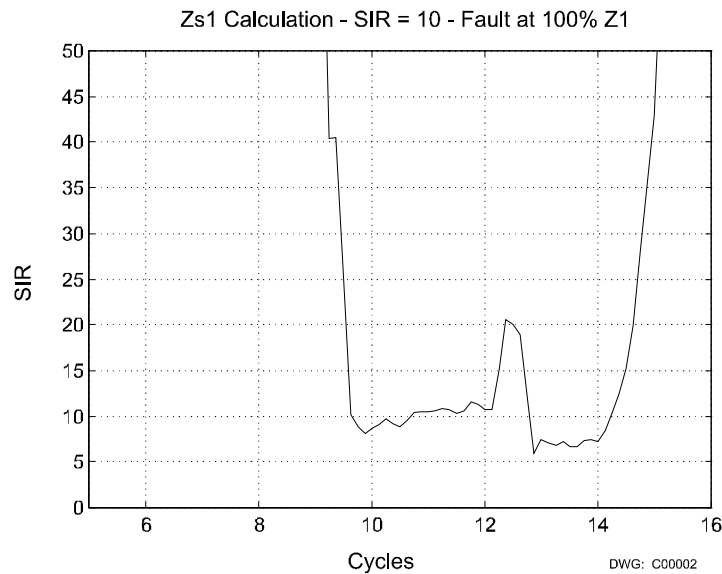


Figure 21: Relay SIR Calculation for an A-Phase-to-Ground Fault at the End of Zone 1 in a System With $SIR = 10$

SECURE MEANS OF IMPROVING TOTAL PROTECTION TRIPPING TIMES

Communications-aided protection systems must detect in-section faults and trip without intentional delay while maintaining security. In this section of the paper, we explore secure means of decreasing the total protection tripping time of a Permissive Overreaching Transfer Trip (POTT) scheme. We define total protection tripping time (TPTT) as the time required to energize breaker trip coils at both ends of the protected line.

Traditional Protection System Tripping Time Evaluation

Figure 23 and Figure 24 show traditional POTT protection system TPTT for phase and ground faults along Line 1 in Figure 22. Relays S and R trip instantaneously using Zone 1 distance elements (set to 85% of the line impedance). Relays S and R time-delay trip and key the permissive channel using Zone 2 distance elements (set to 150% of the line impedance). To increase fault resistance (R_F) coverage, both relays also key the permissive channel and time-delay trip using negative- and zero-sequence directional overcurrent elements set at 0.5 A secondary. Directional control logic for these elements contains load unbalance restraint which prevents the element from picking up for load unbalance. The communications channel in our example is a dedicated fiber-optic link. Other communications channels may yield longer TPTTs.

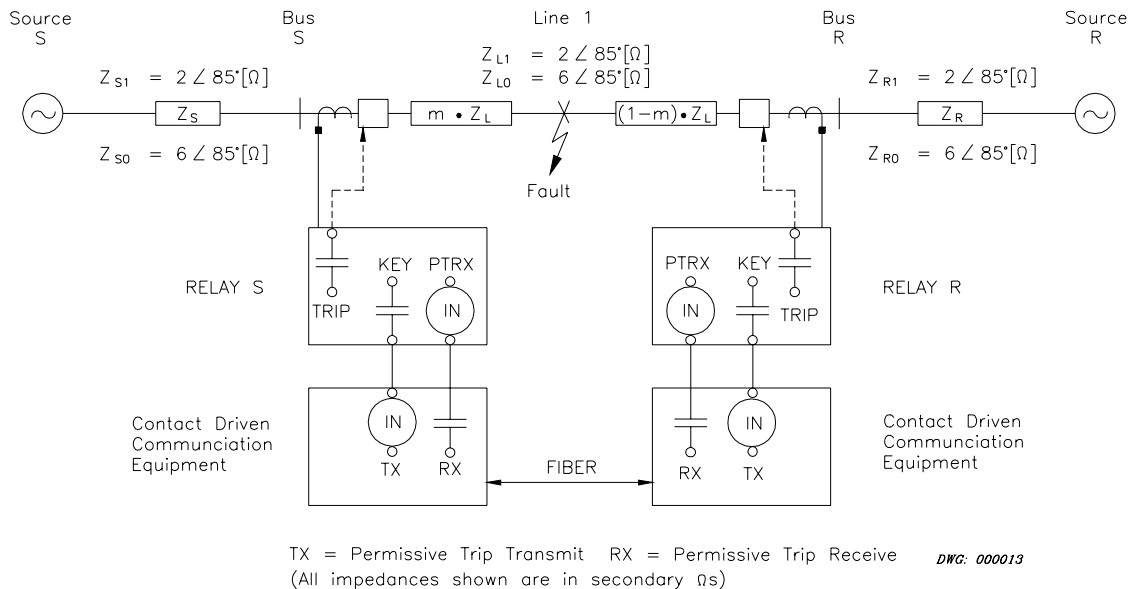


Figure 22: System Single-Line Diagram and Traditional Protection System Block Diagram

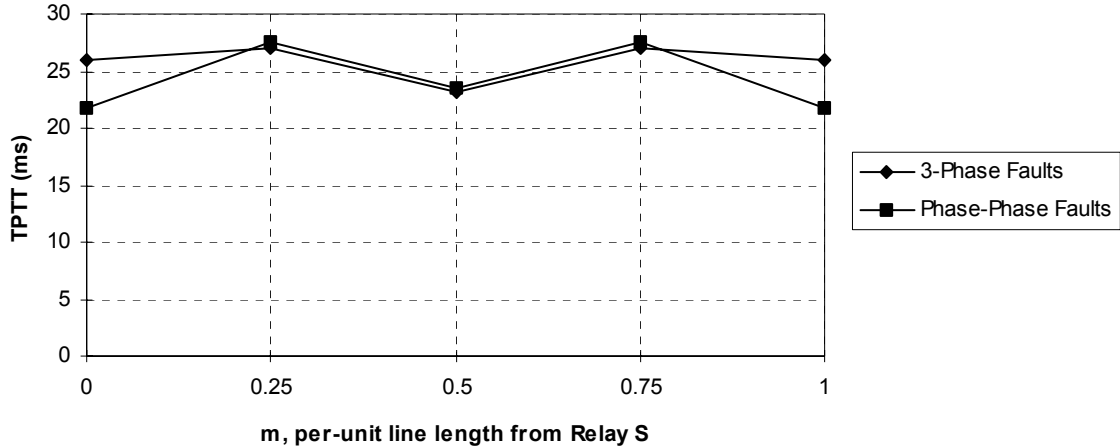


Figure 23: Traditional Protection System Phase Fault TPTTs Without Fault Resistance

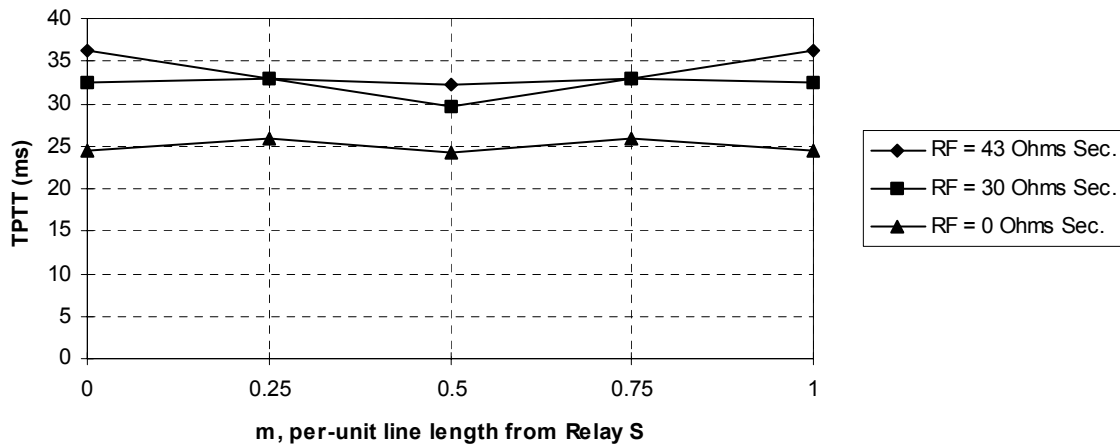


Figure 24: Traditional Protection System Single-Line-to-Ground Fault TPTTs Considering RF

Analysis of the TPTTs shown in Figure 23 and Figure 24 suggest concentrating on the following areas:

1. Decrease the permissive trip (PT) keying delay using separate pilot elements instead of sharing one element for PT keying and time-delayed tripping.
2. Decrease the trip and key output contact operate times.
3. Decrease PT transmit and input contact debounce time using direct digital Relay-to-Relay communication.
4. Decrease the PT keying delay using directional elements.

Figure 25 and Figure 26 show the combined effects of those speed-up techniques. The following sections discuss each technique.

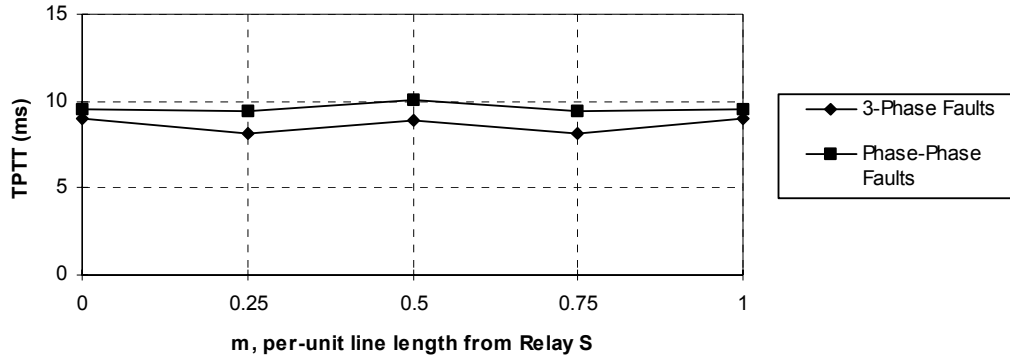


Figure 25: Improved TPTTs for Phase Faults Placed Along Line 1 Without Fault Resistance

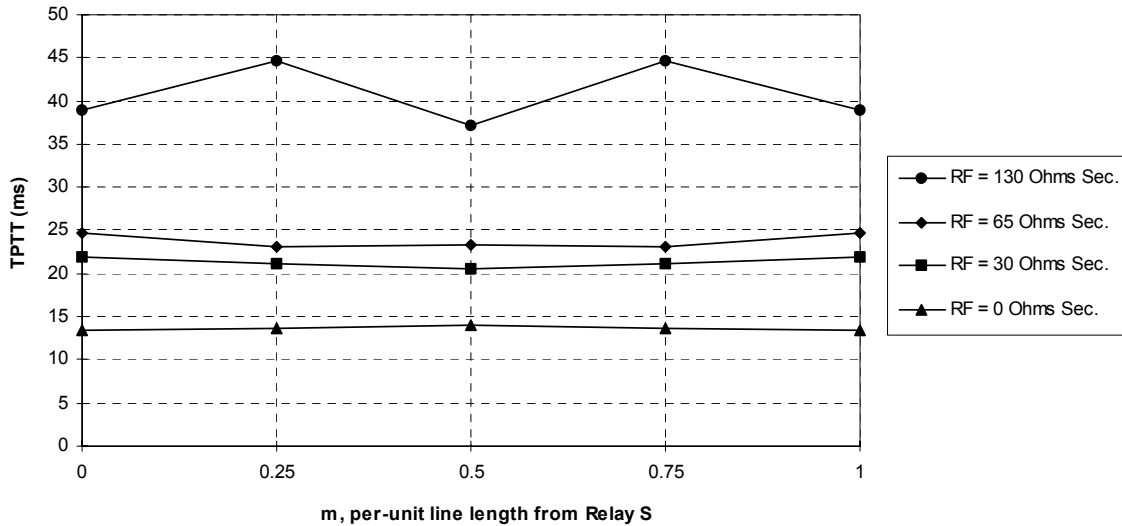


Figure 26: Improved TPTTs for Single-Line-to-Ground Faults Placed Along Line 1 Considering RF

Use Pilot Zone Elements to Decrease TPTT

When the Zone 2 elements used in communications-aided tripping are also used for time-step protection, their reach settings are typically restricted to 120 - 150% of the line impedance. Pilot zones can have much larger reaches.

A distance element with a larger reach operates faster than a distance element with a shorter reach. In microprocessor-based relays, one reason for this operating time difference is the digital filtering of the voltage and current quantities. Reference [8] describes a practical relay design which uses these filtered voltages and currents to calculate the minimum reach setting required for an impedance element to just detect a fault. The minimum reach M is compared against set scalar zone thresholds to determine if that zone of distance protection is picked up.

Figure 27 and Figure 28 show the phase distance M trajectories for Relays S and R after inception of a three-phase fault at $m = 0$ in Figure 22. In this example, we use a one-cycle cosine

digital filter [1]. In both Figure 27 and Figure 28, the rate-of-decrease of M is initially rapid but slows as it approaches the steady-state value.

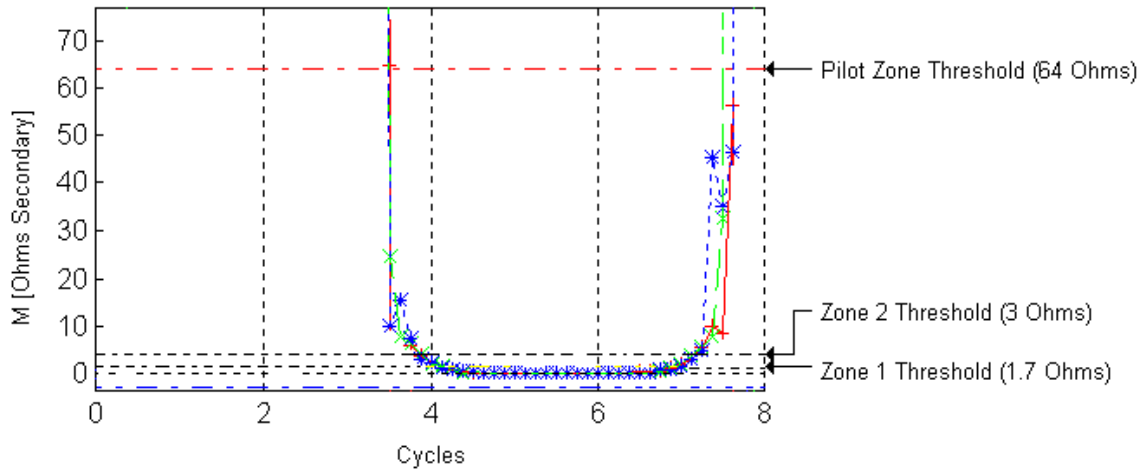


Figure 27: Calculated Phase Distance M Trajectories for Relay S

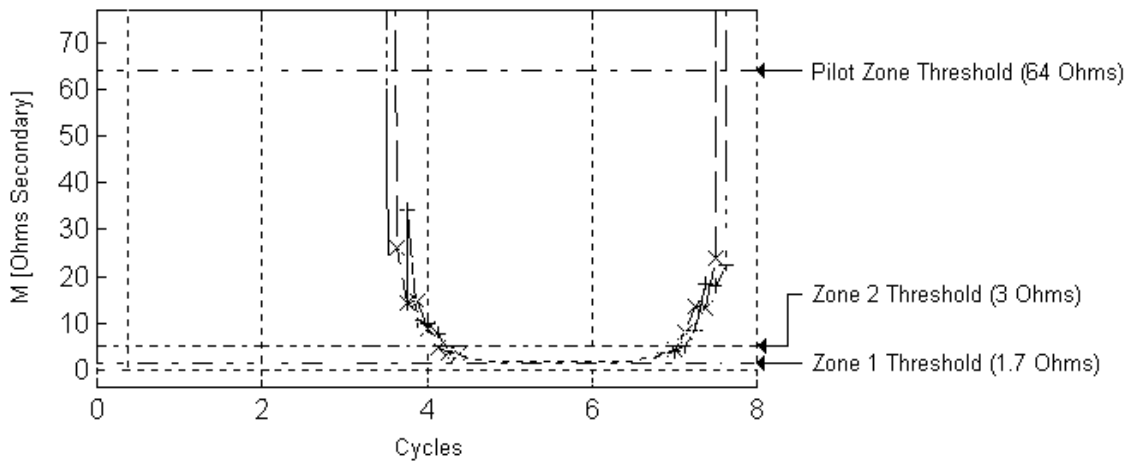


Figure 28: Calculated Phase Distance M Trajectories for Relay R

We do not need to wait for M to arrive at its final steady-state value before keying the permissive channel to the remote terminal if the phase distance elements are secure and the relay includes load encroachment logic. The later requirement ensures that the distance elements are not picked up during heavy load current. Notice that M drops below the pilot zone element threshold of 64Ω secondary about a half-cycle before it drops below the Zone 2 reach of 3Ω . Thus, we can expect to key the permissive channel about a half-cycle sooner using a 64Ω pilot zone. In fact, this change decreases the PT key time for Relay S from 13.4 ms to 7.7 ms. As expected, the Relay R trip time also decreased from 24.3 ms to 17.7 ms. Relay S still trips in 18.8 ms. Using this technique, the remote terminal trips before the local terminal for a close-in three-phase fault.

High-Speed Output Contacts Dramatically Decrease TPTT

In the traditional scheme, almost one-third of the TPTT is spent waiting for contact outputs to change state. Reference [5] describes a new output circuit which reduces contact operating time to less than 10 μ sec. In addition to fast operating speed, and high continuous carry current and isolation voltage, these new output contacts have extremely high interrupt ratings: 10 A at 125 Vdc for a circuit with $L/R = 40$ ms. This interrupt rating exceeds the required rating to make and break trip coil current, and far exceeds the capacitive make and break current associated with energizing communications equipment inputs.

For a three phase fault at $m = 0$ in Figure 22, these high-speed output contacts reduce relay trip times by 3 ms at Bus S and 6 ms at Bus R. With the combination of the pilot zone technique and high-speed output contacts, relays at both line terminals trip before the Zone 1 distance element picks up in the local relay.

Improved Relay-to-Relay Communication Reduces PT Transmit and Receive Delays by Half

Even using high-speed output contacts on both protective relays and communications equipment, the time spent exchanging information in the traditional fiber-based POTT scheme is 4 ms (2 ms for transport delay and 2 ms of debounce time on the PT input at the remote terminal). Relay-to-Relay communication [6] and port-powered fiber-optic transceivers now transmit and receive permissive tripping information in 2 ms at 19200 baud transmit rate. The net reduction in TPTT is 2 ms.

Figure 29 shows the complete communications-aided tripping scheme using Relay-to-Relay communication and fiber-optic transceivers.

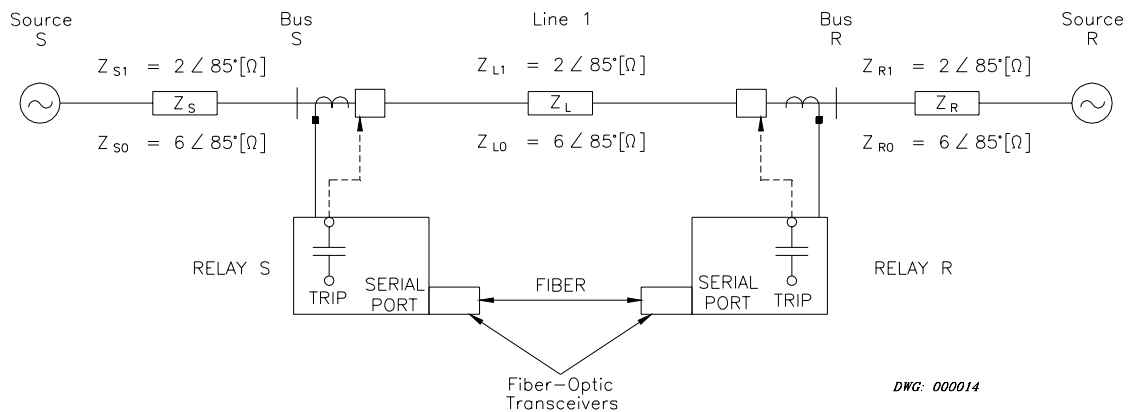


Figure 29: System Single-Line Diagram and Protection System Using Fiber-Optic Transceiver Communications Equipment Block Diagram

Relay-to-Relay Communication Review

Relay-to-Relay communication is a relatively new concept whereby the Bus S and R relays transmit and receive up to eight bits of data over a serial communications link. Each relay sends the status of eight programmable internal relay elements to the remote terminal relay every 2 ms. The integrity of each received message is checked before the relay uses the received element

status. Received data security checks include: CRC (cyclic redundancy check), byte number flag checks, framing error checks, and byte received timing. Each relay treats received and transmitted bits as additional programmable contact inputs and outputs.

Relay-to-Relay Communication Reduces Tripping Delays

Microprocessor-based relays typically read each contact input status once per sampling interval. If the relay sampling rate is 16 times per power system cycle, each input is sampled every 1.04 ms. For physical contact inputs, most relays require the contact input to be in the same state two or more processing intervals before accepting a change-in-state. This is a security measure against dc circuit transients. Because the contact input status data received through the serial port must pass the security checks described above, the protective relay does not require two processing intervals to read a new contact input status. Thus, using Relay-to-Relay communication logic saves 2 ms of contact input read time.

Directional Elements in New Communications-Aided Tripping Scheme Decrease TPTT and Increase R_F Coverage

Using direct digital Relay-to-Relay communication allows us to improve the fault resistance coverage of the protection scheme. Reference [7] describes a new communications-aided protection scheme that offers high-speed clearing of most faults. This same scheme offers better dependability and security than traditional communications schemes. Figure 30 shows the new communications scheme logic.

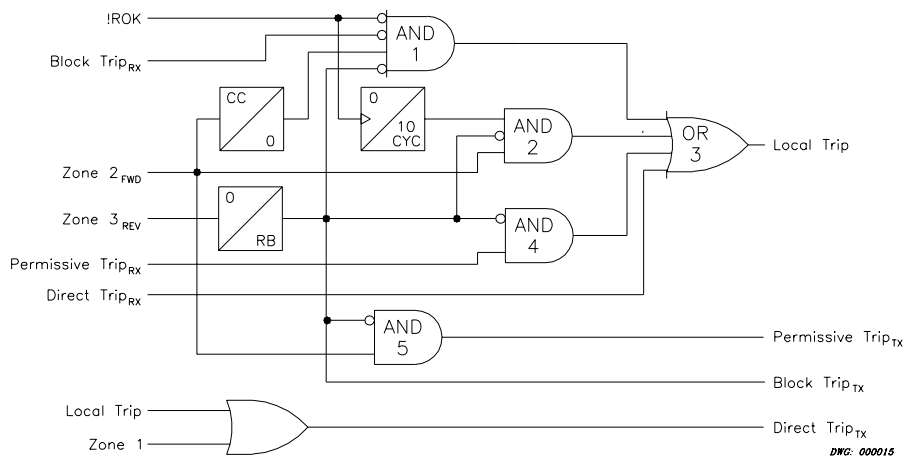


Figure 30: New Communications-Aided Tripping Scheme Logic

We replaced Zone 2 and Zone 3 distance elements in the logic of Figure 30 with directional elements. Because directional elements only discriminate between forward and reverse faults, they are generally faster than distance elements. In fact, these directional elements are typically 2 ms faster than the pilot zone distance element described above.

Figure 25 and Figure 26 combine the directional element-based pilot scheme, direct digital Relay-to-Relay communication, and high speed output contacts. Notice that the TPTT decreased from 24.3 ms to 9.0 ms for a three phase fault at $m = 0$.

SUMMARY

1. A one-cycle FIR filter removes most of the noise from relay input quantities to allow secure impedance calculation. In order to increase relay tripping speed for close-in faults, filters with shorter window length are necessary.
2. The performance of a variable filtering scheme matches the relationship between impedance calculation accuracy and filter window length. It provides decreased tripping times for close-in faults and at the same time maintains its security.
3. Mho element polarization with long memories provides reliable relay operations under challenging fault and system conditions such as zero-voltage three-phase faults and faults with a voltage inversion. However, system frequency excursions present a security problem for long memory polarization. An adaptive polarizing scheme tracks system and fault conditions to provide reliable polarization and reduce the frequency excursion effects.
4. The traditional OOS blocking schemes lack dependability for conditions that evolve to three-phase fault. With the addition of inner blinders and an adaptive timer to the traditional scheme, the new scheme overcomes this limitation.
5. Previous solutions to overcome CVT-transient-induced instantaneous distance element overreach problems assume a fixed SIR. The amount of reach reduction must consider the actual SIR to avoid unwanted tripping delays.
6. Directional element-based pilot schemes significantly reduce fault detection time. Distance element methods achieve the same security, but the directional elements are generally faster.
7. High-speed output contacts capable of making and breaking trip coil current reduce tripping time while increasing protection system reliability.
8. Relay-to-Relay communication logic at 19200 baud decreases TPTT and increases scheme security by eliminating contact-driven communications equipment.

REFERENCES

- [1] E. O. Schweitzer III and D. Hou, "Filtering for Protective Relays," Proceedings of the 19th Annual Western Protective Relay Conference, Spokane, WA, October 1992.
- [2] J.S. Thorp, A.G. Phadke, S.H. Horowitz and J.E. Beehler, "Limits to Impedance Relaying," IEEE Transaction on Power Apparatus and System, Vol. 98, No. 1, 1979.
- [3] E. O. Schweitzer, III, "New Developments in Distance Relay Polarization and Fault Type Selection," Proceedings of the 16th Annual Western Protective Relay Conference, Spokane, WA, October 1989.
- [4] D. Hou and J. Roberts, "Capacitive Voltage Transformers: Transient Overreach Concerns and Solutions for Distance Relaying," Proceedings of the 22nd Annual Western Protective Relay Conference, Spokane, WA, October 1995.
- [5] SEL-352 Instruction Manual, Appendix G, May 1997.
- [6] K. C. Behrendt, "Relay to Relay Digital Logic Communication for Line Protection, Monitoring, and Control," Proceedings of the 23rd Annual Western Protective Relay Conference, Spokane, WA, October 1996.

- [7] E. O. Schweitzer III and J. J. Kumm, "Statistical Comparison and Evaluation of Pilot Protection Schemes," Proceedings of the 23rd Annual Western Protective Relay Conference, Spokane, WA, October 1996.
- [8] E. O. Schweitzer III and J. Roberts, "Distance Relay Element Design," Proceedings of the 19th Annual Western Protective Relay Conference, Spokane, WA, October 1992.

BIOGRAPHY

Daqing Hou received BS and MS degrees in Electrical Engineering at the Northeast University, China, 1981 and 1984, respectively. He received his Ph.D. in Electrical and Computer Engineering at Washington State University in 1991. Since 1990, he has been with Schweitzer Engineering Laboratories, Inc., Pullman, Washington, USA, where he is currently an engineering manager. His work includes system modeling, simulation and signal processing for power system digital protective relays. His research interests include multivariable linear systems, system identification, and signal processing. Hou is a member of IEEE. He has multiple patents and has authored or co-authored several technical papers.

Armando Guzmán received a BSEE degree from Guadalajara Autonomous University (UAG), Mexico, in 1979. He received a Fiber Optics Engineering Diploma from Monterrey Institute of Technology and Advanced Studies (ITESM), Mexico, in 1990. He served as Regional Supervisor of the Protection Department in the Western Transmission Region of Federal Electricity Commission (the electrical utility company of Mexico) for 13 years. He lectured at the Guadalajara Autonomous University in power system protection. Since 1993, he has been with Schweitzer Engineering Laboratories, Inc., Pullman, Washington, where he is currently a research engineer. He is a member of IEEE and has authored and co-authored several technical papers.

Jeff Roberts received his BSEE from Washington State University in 1985. He worked for Pacific Gas and Electric as a Relay Protection Engineer for over three years. In 1988, he joined Schweitzer Engineering Laboratories, Inc. as an Application Engineer. He now serves as the Research Engineering Manager. He has written many papers in the areas of distance element design, sensitivity of distance and directional elements, directional element design, and analysis of event report data. Mr. Roberts holds multiple patents and has other patents pending. He is also a member of IEEE.